# Machine Learning Classification of Maladaptive Rumination and Cognitive Distraction in Terms of Frequency Specific Complexity

Serap Aydın

*Hacettepe University, Medical Faculty, Biophysics Department, Ankara, Turkey*

Barış Akın *(student)*

*Hacettepe University, School of Medicine, Ankara, Turkey*

## Abstract

In this study, cognitive and behavioral emotion regulation strategies (ERS) are classified by using machine learning models driven by a new local EEG complexity approach so called Frequency Specific Complexity (FSC) in resting-states (eyes-opened (EO), eyes-closed (EC)). According to international 10-20 electrode placement system, FSC is defined as entropy estimations in Alpha $(8-12\ Hz)$ and Beta $(12.5-30\ Hz)$ frequency band intervals of non-overlapped short EEG segments to observe local EEG complexity variations at 62 points on scalp surface. The healthy adults who use both rumination and cognitive distraction frequently are included in the 1st groups, while the others who use these strategies rarely are included in the 2nd group with respect to Cognitive Emotion Regulation Questionnaire (CERQ) scores of them. EEG data and CERQ scores are downloaded from publicly available data-base LEMON. In order to test the reliability of the proposed method, five different supervised machine learning methods in addition to two Extreme Learning Machine models are examined with 5-fold cross-validation for discrimination of the contrasting groups. The highest classification accuracy (CA) of 99.47% is provided by Class-specific Cost Regulation Extreme Learning Machines in EC state. Regarding cortical regions (anterio-frontal, central, temporal, parieto-occipital), the regional FSC estimations did not provide the higher performance, however, corresponding statistical distribution shows the decrease in EEG complexity at mostly anterior cortex in the 1st group characterized by maladaptive rumination. In conclusion, FSC can be proposed to investigate cognitive dysfunctions often caused by the use of rumination.

*Keywords:* EEG complexity, brain biophysics, emotion regulation, entropy, machine learning

*Email address:* `drserapaydin@hotmail.com; serap.aydin@hacettepe.edu.tr` (Serap Aydın)

## 1. Introduction

The recent attractive research studies combines computer science aspects with cognitive neuroscience [1, 2, 3, 4]. This bridge provides new opportunities in order to develop decision-making systems with artificial intelligence models in both medical and social sciences. Quantitative neuromarkers/indicators have been estimated from brain waves measured as Electro-Encephalo-Graphy (EEG) series according to several goals such as decoding the instant thoughts of disabled people about the action they need [6, 7, 8], recognizing an emotional state [9, 10, 11], investigating attentive decision-making skills [12, 13], measuring psychiatric well-being [14, 15, 5].

The motivation of the present study is to propose a new metric, Frequency Specific Complexity (FSC) for classification of two contrasting cognitive groups consisting of people who use a negative emotion regulation strategy (ERS), rumination frequently and those who rarely use it. FSC is defined as averaged neuronal complexity in Alpha $(8 - 12\ Hz)$ and Beta $(12.5 - 30\ Hz)$ frequency bands of short EEG segments at resting-state. Approximate Entropy (AE) and Wavelet Entropy (WE) have been examined to estimate neural complexity levels in both eyes-closed (EC) and eyes-opened (EO) states and then the resulting FSC values are classified by using machine learning models with respect to cortical regions. EEG data is downloaded from a publicly available database called LEMON described in reference [23]. The groups are organized in accordance with the individuals' scores on Cognitive Emotion Regulation Questionnaire (CERQ).

EEG recordings provide prompt and objective information in extracting meaningful and accurate markers/indicators about both cognitive process and emotional states as well as mood [16, 17]. ERS refers the ability to control both formation and behavioral responses of emotions according to one's location and time. Behavioral and cognitive managements can be referred as control of anxiety, reducing the stress, handling difficult emotions, etc... Thus, emotion management skills referring which ERS is used frequently, plays an important role in every field of life [18]. Association of different cognitive ERS with brain activities has become an attracting research topic in recent years. In detail, the main two opposite categories of CERS are rumination and distraction [19]: Rumination is an emotion-oriented regulation strategy meaning to focus on depressive behaviors and thoughts, thereby increasing the negative effects of depressive symptoms. On the contrary, distraction is a strategy that directs one's attention to pleasant thoughts and actions that can distract from the negative subject in order to get away from the depressive mood [20, 21]. Even if neuroimaging modalities have been examined in estimating differences among CERs in response to emotional stimuli [22], no study has been published on cross-correlation between spontaneous neuro-cortical complexities and contrasting CERs to date. In the present study, it is the first time to estimate local complexity levels from resting state EEG recordings to discriminate maladaptive

ruminative thoughts in healthy adults. In order words, two contrasting cognitive skills (positive and negative ERSs, i.e. rarely and frequently use of rumination) are indicated by FSC levels in both EC and EO states in order to investigate the impact of ruminative thoughts on spontaneous postsynaptic potentials embedded in resting-state EEG recordings, since the case of open and closed eyes in decoding cognitive deficits depending on the presence of psychiatric disorders [24, 25, 27].

Moderate neuro-functional abnormalities can be detected through EEG analysis, since this modality provides to observe and store superimposed electrochemical current contributions from all synchronized neurons within a volume of brain tissue (i.e. near to electrode placement). Comparing neuro-imaging methods, extraction of quantitative markers from EEG measurements provide superior diagnostic tools to the neuroscientist due to its temporal resolution yield relevant information about electrical activities of local neuronal networks [28, 29]. Depending on experimental paradigm, domain specific different non-linear methods have been applied to EEG recordings in recognizing of neuro-developmental (Autism Spectrum Disorder) [30], and neuro-degenerative (Alzheimer's disease) [31] even estimate neurological dysfunctions such as epilepsy [32, 33] and seizure [34, 35]. In diagnosis, the severity of disease is another and secondary target of smart classifiers. Different from clinical applications, other crucial goal of advanced EEG classification is to understand higher-order brain functions such as attention [36], and consciousness [37, 38].

FSC has been defined as mean neural complexity associated with alpha ($8 - 12\ Hz$) and beta ($12.5 - 30\ Hz$) sub-bands of resting-state EEG segments for detection of cognitive skills in the present study. Approximate Entropy (AE) and Wavelet Entropy (WE) are compared to each other to obtain frequency-band specific entropies of stimulus-free EEG recordings in eyes-opened and eyes-closed states in two contrasting groups including frequently and rarely use of rumination and distraction in adults (women and men together). Due to non-linear, non-periodic and non-deterministic nature of EEG series, the primary step of the propose method is to apply well-arranged finite-impulse-response (FIR) filters to non-overlapped short EEG segments of 2 $sec$ in order to extract alpha and beta sub-bands in both EO and EC states.

AE is the mostly examined embedding entropy approach in diagnostic EEG analysis [48, 49]. WE has been mostly used to decompose the signal into frequency components in brain-computer interfaces driven by evoked brain waves in response to an external stimuli [50]. To compute WE, discrete or continuous Wavelet Transform (WT) have to be applied to signal segments. Continuous WT was found to be sensitive to phase correlation of two cortical regions in neurological diseases such as non-convulsive epileptic seizure [32] and Obsessive Compulsive Disorder [51]. Discrete WT has been applied to not only ongoing spontaneous EEG but also evoked brain potentials in response to external stimuli with many different goals such as seizure detection [52], noise reduction [53], anesthesia monitoring [54], and, emotion recognition [55]. Different from these papers, average power of WT coefficients associated with alpha and beta sub-bands, reveals the correlation between wavelet energies and individual per-

3

sonality differences in attentional breadth [56]. In the present study, Discrete WT is applied to alpha and beta sub-bands at a single scale where the particular EEG sub-bands are extracted from pre-processed short segments (applied Notch filter) by using well-oriented FIR filters.

In both clinical applications and neuro-cognitive research, alpha sub-band has provided meaningful indicators in analysis of resting-state EEG recordings in EO and EC states [39]. In more recent studies, both alpha and beta sub-bands have been found to be functional significance with attentional and inhibitory processes in both EC and EO states [108]. Many other research studies have showed that controls can be discriminated from psychiatric disorders such as depression, bipolar, schizophrenia in alpha and beta sub-bands of resting-state EEG in EO [41]. Therefore, alpha and beta sub-band specific entropies are averaged to define FSC in resting-state EEG analysis in the present study.

The usefulness of the proposed cognitive neuro-markers has been tested by using machine learning models driven by five features sets including EEG complexity estimations from the whole cortex and cortical regions (anterio-frontal, central, temporal, parieto-occipital) in classifying two groups having contrasting CERs. Feature extraction and compatible intelligent classification of the features are common and unavoidable steps in both computational and behavioural neuroscience. Embedding entropy concept has been commonly found to be sensitive to quantitative EEG complexity originated from superimposed post-synaptic potentials at a small neural population in particular symptoms of consciousness disorders [42, 43], cortical lesions [44] and sleep cycles [45] in feature extraction step. Entropy based various algorithms have also been applied to EEG recordings in response to affective stimuli for recognition of emotional states [46, 47].

Considering the EEG classification step, the most popular machine learning model is Support Vector Machine (SVM) in extracting quantitative markers from EEG recordings due to its theoretical capability in implicitly detecting complex non-linear interactions between dependent and independent variables [57, 58, 59]. Besides, the performance of SVMs are frequently compared with non-linear and non-parametric classifiers called k-Nearest Neighbors (kNNs) in brain research [60, 61]. In epileptic seizure detection, k-NN has also be compared with Gaussian Naive Bayes (GNB) that is a probabilistic classifier based on Bayesian theory with assumptions of each feature of a particular class is independent of any other feature and the likelihoods are Gaussian [62]. Different from SVMs and kNNs, LR is statistical learning model described as pattern recognizer in several studies focused on different goals such as automated detection of epileptic waveforms [67, 68] and emotion recognition [69] as well as investigation of healthy motor task responses [70]. In recent brain-computer-interface applications, classification performances of both SVM and LR have been compared to Multi Layer Perceptron (MLP) using gradient descent in training with the gradients calculated using Backpropagation [71]. MLP has also been used for classification of sleep and wakeful states identified by EEG features [72]. Conceptually, SVM and kNN differ from LR in offering multiple training algorithms for classification of electrophysiological features [73]. Commonly GNB

and MLP are generally found to be useful in small feature set [72, 62]. In the present study, those popular five machine learning models have been used for discrimination of cognitive ER management capabilities in adults and then their performances are compared to each other with respect to neuro-cortical complexity features, i.e. FSC estimations.

The novelty of the present study is to propose a new EEG based local complexity indicator for fast and robust detection of negative emotion regulation strategy so called maladaptive rumination from resting-state surface EEG recordings. Both robustness and reliability of the proposed method, Frequency Specific Complexity, have been satisfied by using seven different Machine Learning models with 5-fold cross validation for classification of adults who use contrasting cognitive ERS. The findings provide to understand neural mechanism underlying repetitive negative thoughts triggered by depressive feelings. Since the best performance has been provided by the largest feature set including FSC estimations across the whole cortex, the results are found to be meaningful and consistent with cognitive neuroscience hypotheses, as rumination requires both cognitive and emotional subprocesses associated with the activation of multiple and diverse brain regions responsible for attention, self-referential processing, and recall of autobiographical memories [63].

## 2. Methods

### 2.1. The Participants

Surface EEG measurements and the psychometric test scores of the participants were obtained from an internationally validated, accessible database, LEMON introduced in reference [23]. In collecting data, primary step was to complement cognitive test batteries lasting about 4 hours of duration each at first day. Resting-state EEG series were recorded from participants who completed Cognitive Emotion Regulation Questionnaire (CEQR) at second day. As well, psychiatric interview was done by experts with the participants to decide the healthy status of them. So, hypertensive patients and those with cardiology and neurological diseases are not included.

Raw data was analysed in the present study. 62-channel EEG measurements were categorized according to CEQR scores of the individuals. CERQ measures how often individuals use rumination (I) and cognitive distraction (II) strategies, with sub-scales of rumination and positive refocusing into 36 questions on a 5-point Likert scale (1 refers 'almost never' to 5 refers 'almost always') [74].

Group-1 included the individuals use both strategies I and II frequently (13 women, 7 men), while Group-2 included the individuals rarely use any of the strategies I and II (6 women, 14 men). In detail, the individuals (aged between 20 to 65) scaled high rumination tendencies as well as high distraction tendencies of CERQ with respect to mean (5.40) and std (2.62) values in Group-1, while the individuals scaled low rumination tendencies as well as low distraction tendencies of CERQ scores with respect to mean (4.90) and std (2.58) values in Group-2. The quantitative scales were determined by adding and subtracting
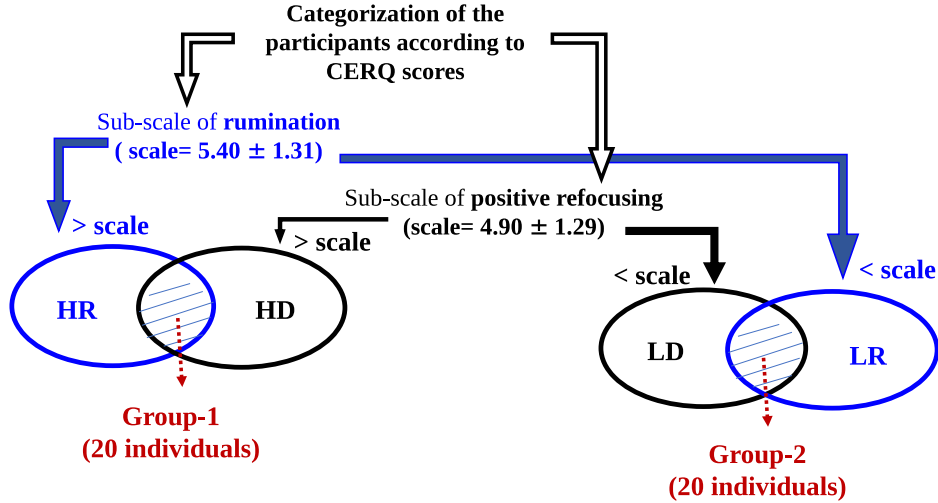
Figure 1: Schematic representation of group categorization depending on individuals' response to CERQ where HR (High-Rumination) refers frequently use of rumination, LR (Low-Rumination) refers rarely use of rumination, HD (High-Distraction) refers frequently use of distraction, LD (Low-Distraction) refers rarely use of distraction

half of standard-deviation to the mean value among all individuals. Schematic representation of this categorization is presented in Figure 1.

### 2.2. EEG Data Acquisition and Pre-processing

Brain Products ActiCaps (GmbH, Gilching, Germany) was used to measure 62-channel surface EEG series from scalp surface of the awake volunteers who were not assigned any task and sat in a comfortable chair in a resting-state. Multi-channel recordings (61 scalp electrodes in addition to VEOG below the right eye) were stored into 16 blocks (8 blocks in eyes-opened (EO) and 8 blocks in eyes-closed (EC) states). These recording blocks were organized with presentation software (Neuro-behavioural Systems Inc., Ver16.5, Berkeley, USA). In order to ensure the state of EO or EC, the participants looked at computer screen (black cross presented on a white background). The length of each bloc was 60 $sec$.

EEG recording electrodes were placed on scalp with respect to the international 10–20 extended electrode placement system where the reference electrode was linked to FCz and the ground was located at the sternum. The amplitude resolution was 0.1 $\mu Volt$. Electrode impedance was kept below 5 $k\Omega$. EEG data was digitized with the sampling frequency of 2500 $Hz$, however, down-sampling was applied to the data with 250 $Hz$. The down-sampled raw data was firstly extracted from the data-base through a Pyhton code given as Appendix. During extraction of the raw data, 16 data blocks, interleaved to each other in a single file, were separated for each individual. Then, the physiological artifacts were

removed from raw data, i.e. unprocessed EEG data recordings data as proposed in the reference study [65] according to the known frequency components (lower than 4 $Hz$) of the artifacts originated from eye blinks [64]. EEG filtering and analysis were performed in MATLAB2021Ra by using three main toolboxes as Signal Processing Toolbox, Statistics and Machine Learning Toolbox.

Figure 2 shows the schematic representation of EEG analysis. For each participant in each group, network noise at 60 $Hz$ was removed from non-overlapped consecutive short EEG segments of 2 $sec$ through an Infinite-Impulse-Response (IIR) filter with order of 35 (Notch filtering). The corresponding specifications of this filter were optimized as described in reference [66].

## 3. Frequency Specific Complexity

Frequency Specific Complexity (FSC) has been estimated from pre-filtered short EEG segments across 62-channel recordings in both EO and EC states in groups. A finite-impulse-response (FIR) filter was applied to EEG segments, filtered by IIR, to extract frequency band intervals. Regarding optimized FIR filter specifications, the filter order was 35 with the density factor of 20 where the bandwidth (BW) was wo/354 (wo=60/Fs/2). The sub-band ripples were 0.05750 and, stop-band attenuation was 0.0001. The frequency intervals were $8 - 12\ Hz$ and $12.5 - 30\ Hz$ in extracting alpha and beta sub-bands, respectively.

Considering frequency sub-band of EEG segment ($s$) is denoted by $x_{sub-band} = [x(1)x(2)...x(N)]$, Approximate Entropy (AE) is defined in form,

$$AE_x = \phi_m(r) - \phi_{m+1}(r) \tag{1}$$

where $\phi_m(r) = mean(\ln(C_r^m(i)))$. A sliding window with length of an embedding dimension of $m$, is applied to the sequence of $x_{sub-band}$ in order to consider statistical variations throughout the sequence within a tolerance $r$ based on logarithmic likelihood [75, 76].

$$C(x) = \frac{1}{N-m} \sum_{i=1}^{N-m} L(i) \tag{2}$$

Here, $L(i) =\ number\ of\ d[x_{m+1}(i), x_{m+1}(j)] \leq r$. The small tolerance level can be considered as noise threshold in a random process. In applications this threshold is predefined as $r = 0.25std(x)$. The useful embedding dimension, $m$ is estimated by calculating the false nearest neighbor as described in reference [78]. AE is computed for both alpha and beta sub-bands by using equation 1 and then, mean value of these estimations is defined as FSC in form,

$$FSC_s = \frac{AE_{alpha} + AE_{beta}}{2} \tag{3}$$

Wavelet Entropy (WE) is introduced as a complexity measure [79]. WE is applied to frequency sub-bands of short EEG segments for estimation of the degree of randomness in specified sub-bands in form,
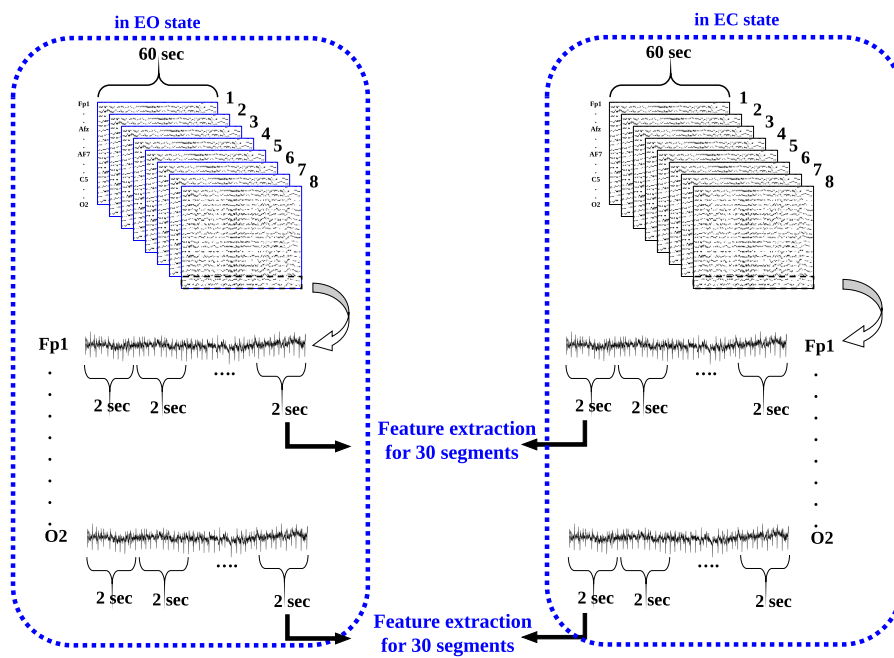
7

Figure 2: Algorithmic steps in EEG analysis before applying EEG complexity metrics to short EEG segments

$$WE = -\sum p_j \ln (p_j) \tag{4}$$

where $p_j$ refers probability distribution that can be considered as a time-scale density. In estimating WE, $p_j$ is given by,

$$p_j = \frac{E_j}{E_t} \tag{5}$$

Here, $E_j$ and $E_t$ denote relative and total wavelet energies that are extracted from Discrete Wavelet Transform (DWT) coefficients as introduced in [79]. The corresponding wavelet coefficients are assumed to be local residual errors between successive signal approximations at scales $j$ and $j + 1$. In the present study, $j$ is set to 1, since WE is computed for frequency sub-bands of short EEG segments. In examining DWT, Daubechies-5 ($db - 5$) is chosen as Mother Wavelet function due to their non-symmetric, orthogonal and compact support nature similar to resting-state short EEG recordings [80, 82]. The reference paper presents a detailed review on the studies that apply WE to EEG recordings in mental disorders [81]. In the present study, WE is computed for both alpha and beta sub-bands by using equation 1 and then, mean value of these estimations is defined as FSC in form,

$$FSC_s = \frac{WE_{alpha} + WE_{beta}}{2} \tag{6}$$

*3.1. Classification of Groups*

Five different supervised machine learning methods as Logistic Regression (LR), Support Vector Machine (SVM), k-Nearest Neighbours (kNN), Gaussian Naive Bayes (GNB), Multi Layer Perceptron (MLP) and two Extreme Learning Machine (ELM) models as single-layer ELM and Class-specific cost regulation ELM (CCR-ELM) were used for classification of two balanced groups with respect to five particular feature sets as follows:

- SET-1 includes FSC levels extracted from 62-channel recording sites

- SET-2 includes FSC levels extracted from anterio-frontal recording sites (Fp1, Fp2, AF3, AF4, AF7, AF8, F1, F2, F3, F4, F5, F6, F7, F8)

- SET-3 includes FSC levels extracted from central sites (FC1, FC2, FC3, FC4, FC5, FC6, C1, C2, C3, C4, C5, C6, CP1, CP2, CP3, CP4, CP5, CP6),

- SET-4 includes FSC levels extracted from temporal sites (FT7, FT8, T7, T8, TP7, TP8)

- SET-5 includes FSC levels extracted from parieto-occipital sites (P1, P2, P3, P4, P5, P6, P7, P8, O1, O2, PO3, PO4, PO7, PO8, PO9, PO10)

9

Group-1 and Group-2 were labeled by 0 and 1, respectively in two-class binary classification steps. The feature sets were obtained in both EO and EC states, separately. The features were extracted from the raw data. In both EO and EC states, 8 blocks in EEG recordings of 60 *sec* were analysed for each participant. Data was segmented through a constant sliding window of 2 *sec* in each block. Therefore, the total number of features is 297.600 (62 (recording channels) $x$ 8 (blocks) $x$ 30 (segments) $x$ 40 (subjects) = 595.200) in the largest feature set. The number of features was identical in groups according to cortical regions identified by particular feature sets above. Thus, the groups were balanced in classification step.

Scikit-Learn Machine Learning Library was used to implement the classifiers with 5-fold Cross-Validation in Python3.7.12. In detail, the kernels were chosen as Radial Basis Functions in examining of SVMs according to the suggestions in medical applications [84]. ELM was implemented with multiple layers of hidden nodes having the parameters need not be tuned [83]. In addition, CCR-ELM was also implemented for two-class classification due to its reported superiority to ELM [112, 113]. The configuration parameters were optimized by using Adaptive Moment Estimation Method (Adam) in MLP. The Grid-Search method was used to find the optimum parameters in both conventional ELM and CCR-ELM algorithms of single-hidden layer feed-forward neural networks with sigmoidal activation function. The optimum variables were determined by using Grid-Search method in another machine learning models, as well. Commonly, the well known performance metrics called as Classification Accuracy (CA), Area-Under-Curve (AUC), F1-score and G-mean were computed in applications. The reference study presents the mathematical definitions of these error criteria [85].

## 4. Related Works

In cognitive neuroscience, the maladaptive and detrimental consequences of focus on depressed mood have been frequently studied in order to show the association of negative self-focus with depression [87, 88, 89]. Several studies provided the evidence suggesting that rumination tendency is associated with self-reported generalized anxiety symptoms [92] and post-traumatic stress [93]. Thus, rumination has been considered as an important etiological variable of depression [90], however, the later study defines the rumination with a vital trans-diagnostic factor in emotional disorders [91]. Therefore, the common goal of the most of the related research studies is to discuss the role of impaired working memory on rumination-related cognitive mechanisms according to EEG [96, 95, 97, 98]. A few studies has been presented to relate f-NIRs indicators with rumination in response to go/no go task driven by emotional stimuli [99]. Besides, EEG neuro-feedback protocol has also been proposed to treat depression and rumination in more recent studies [94].

Ruminations can be defined as repetitive thoughts associated with consequences of one's negative/depressive feelings. The present study examines FSC

levels of neuronal populations over scalp in maladaptive rumination at resting-state in order to show the relations between spontaneous neurotransmitter activities embedded in surface EEG measurements with resting-state maladaptive rumination without any task and/or stimulus. So, default-mode brain functions are analyzed with respect to cortical regions. For this purpose, AE and WE are used to compute FSC in frequency band intervals of both EO and EC states in two groups having the identical number of EEG features. The balanced groups were classified with machine learning models.

## 5. Results

Two groups were classified with respect to features sets including FSC estimations and the resulting classification performance metrics were listed in tables. In accordance with the use of WE in computing FSC values from resting-state EEG segments at EO and EC states in Tables 1 and 2, respectively. Tables 3 and 4 included the classification performances of the classifiers with respect to feature sets obtained through use of AE in EO and EC states, respectively.

Regarding both Tables 1 and 2, useful CA was provided by SVMs driven by SET1 in both EO and EC states, while none of the other feature sets provided high classification performance (higher than CA of 85%) in any case (EC, EO).

Regarding both Tables 3 and 4, the classifiers produced the perfect performance (CA higher than 90%) in both EO and EC states when SET-1 was considered. Besides, four classifiers (SVM, kNN, ELM, CCR-ELM) provided high CA in both states in considering both SET-2 and SET-3. In detail, kNN and SVM both provided high classification performance in examining each feature set in EC state, while the highest CA of 99.47% was provided by CCR-ELM in examining SET-1 in EC state.

Since, using AE in computing FSC provided clearly better classification of two-groups at both states (EC, EO), the statistical box plots of AE driven FSC estimations were shown as follow: Figures 3 and 5 showed distribution of FSC values in Group-1 at EO and EC states, respectively, while Figures 4 and 6 showed distribution of FSC values in Group-2 at EO and EC states, respectively. Commonly, white boxes refer the left recording channels, black filled boxes refer the corresponding right recording channels, the circulus refer the outliers in those figures. Comparing these figures to each other, the relatively lower EEG complexity levels were produced by Group-1 in both states (EO and EC). In both groups, EEG complexity levels were decreased at EC state.

Between two groups, statistically meaningful and significant differences were obtained by using statistical permutation test as listed in Table 5. Regarding FSC estimations with AE, significant statistical differences between groups were stated at mostly frontal, centro-parietal and parietal locations in both EO and EC states, however, the more electrode placements provided statistically meaningful differences in EO state. The statistical p-values were converted into colored relative scales according to 62-channel EEG electrode placement coordinates as shown in Figure 7.

Table 1: Classification performance results in accordance with FSC estimations with WE at EO state

| Features | Classifier | CA | AUC | F1- score | G-mean |
|---|---|---|---|---|---|
| SET-1 | SVM | **90.62** | 90.64 | 90.63 | 82.15 |
| | kNN | 84.89 | 84.84 | 85.57 | 71.87 |
| | GNB | 61.71 | 62.72 | 48.78 | 31.75 |
| | LR | 77.60 | 77.65 | 77.95 | 60.28 |
| | MLP | 83.59 | 83.60 | 83.72 | 69.87 |
| | ELM | **86.19** | 85.96 | 84.48 | 73.47 |
| | CC-ELM | 80.98 | 81.13 | 81.14 | 65.73 |
| SET-2 | SVM | 82.55 | 82.67 | 78.40 | 62.22 |
| | kNN | 78.90 | 78.88 | 81.34 | 67.74 |
| | GNB | 55.72 | 55.22 | 81.34 | 67.74 |
| | LR | 61.97 | 61.91 | 59.89 | 38.15 |
| | MLP | 70.05 | 69.86 | 72.29 | 48.47 |
| | ELM | 73.95 | 74.01 | 72.68 | 54.48 |
| | CC-ELM | 70.83 | 70.79 | 72.14 | 49.96 |
| SET-3 | SVM | 76.30 | 75.91 | 72.67 | 56.53 |
| | kNN | 73.95 | 73.77 | 71.75 | 54.16 |
| | GNB | 64.58 | 63.43 | 78.50 | 64.69 |
| | LR | 68.75 | 68.36 | 64.07 | 45.63 |
| | MLP | 72.13 | 71.91 | 69.52 | 51.36 |
| | ELM | 81.25 | 81.66 | 80.54 | 66.06 |
| | CC-ELM | 75.26 | 75.37 | 73.68 | 56.30 |
| SET-4 | SVM | 69.79 | 70.19 | 67.60 | 46.65 |
| | kNN | 67.70 | 67.46 | 67.20 | 47.83 |
| | GNB | 54.68 | 53.96 | 59.15 | 40.24 |
| | LR | 53.38 | 53.18 | 54.45 | 31.52 |
| | DNN | 57.55 | 57.35 | 59.95 | 37.65 |
| | ELM | 71.87 | 71.81 | 73.13 | 51.45 |
| | CC-ELM | 70.31 | 70.03 | 72.73 | 48.88 |
| SET-5 | SVM | 69.53 | 69.21 | 65.69 | 47.15 |
| | kNN | 77.08 | 76.99 | 75.82 | 59.23 |
| | GNB | 58.07 | 56.84 | 82.08 | 69.43 |
| | LR | 63.02 | 62.34 | 63.61 | 45.48 |
| | MLP | 63.02 | 62.95 | 57.49 | 38.02 |
| | ELM | 72.39 | 72.35 | 70.88 | 52.34 |
| | CC-ELM | 73.17 | 72.39 | 68.31 | 51.55 |

Table 2: Classification performance results in accordance with FSC estimations with WE at EC state

|  | Classifier | CA | AUC | F1- score | G-mean |
|---|---|---|---|---|---|
| SET-1 | SVM | **89.32** | 89.14 | 88.39 | 79.31 |
| | kNN | **88.54** | 88.52 | 88.83 | 78.35 |
| | GNB | 63.28 | 61.97 | 50.18 | 33.24 |
| | LR | 78.12 | 78.02 | 76.67 | 60.84 |
| | MLP | **87.23** | 87.27 | 86.72 | 76.16 |
| | ELM | 78.90 | 78.92 | 79.28 | 62.29 |
| | CC-ELM | 83.59 | 83.64 | 83.46 | 69.90 |
| SET-2 | SVM | 77.60 | 77.64 | 77.49 | 60.26 |
| | kNN | 77.34 | 77.11 | 74.64 | 58.72 |
| | GNB | 54.68 | 53.86 | 80.33 | 66.13 |
| | LR | 60.93 | 60.46 | 64.09 | 45.44 |
| | MLP | 65.36 | 65.23 | 63.16 | 42.42 |
| | ELM | 76.56 | 76.70 | 76.06 | 58.63 |
| | CC-ELM | 74.21 | 74.28 | 72.73 | 54.79 |
| SET-3 | SVM | 83.85 | 83.81 | 82.29 | 69.53 |
| | kNN | 80.98 | 80.96 | 80.11 | 65.40 |
| | GNB | 59.37 | 59.22 | 76.08 | 60.52 |
| | LR | 69.01 | 68.93 | 63.61 | 45.42 |
| | MLP | 75.52 | 76.14 | 75.00 | 57.34 |
| | ELM | 75.52 | 75.55 | 74.87 | 56.97 |
| | CC-ELM | 83.33 | 83.20 | 82.12 | 69.17 |
| SET-4 | SVM | 71.87 | 71.54 | 75.45 | 49.57 |
| | kNN | 71.35 | 71.35 | 71.94 | 50.92 |
| | GNB | 53.90 | 54.86 | 80.00 | 64.76 |
| | LR | 57.81 | 58.48 | 69.44 | 50.57 |
| | MLP | 63.28 | 62.95 | 60.18 | 41.38 |
| | ELM | 71.09 | 71.35 | 50.81 | 71.90 |
| | CC-ELM | 77.34 | 77.43 | 76.29 | 59.94 |
| SET-5 | SVM | 80.20 | 80.20 | 80.10 | 64.33 |
| | kNN | 78.38 | 78.38 | 78.33 | 61.44 |
| | GNB | 60.41 | 60.25 | 79.88 | 66.15 |
| | LR | 65.10 | 65.04 | 60.82 | 41.19 |
| | MLP | 71.35 | 71.38 | 72.91 | 50.59 |
| | ELM | 67.18 | 67.34 | 64.00 | 44.37 |
| | CC-ELM | 76.56 | 76.57 | 77.04 | 58.58 |

Table 3: Classification performance results with respect to FSC estimations with AE at EO state

|       | Classifier | CA    | AUC   | F1- score | G-mean |
|-------|------------|-------|-------|-----------|--------|
| SET-1 | SVM        | **96.35** | 96.27 | 95.95     | 92.67  |
|       | k-NN       | **98.17** | 98.17 | 95.95     | 92.67  |
|       | GNB        | 64.58 | 64.81 | 58.78     | 59.74  |
|       | LR         | **90.88** | 90.87 | 91.09     | 82.56  |
|       | MLP        | **91.92** | 91.92 | 92.19     | 84.50  |
|       | ELM        | **97.65** | 97.70 | 97.60     | 95.52  |
|       | CC-ELM     | **97.13** | 97.11 | 96.95     | 94.30  |
| SET-2 | SVM        | **92.18** | 92.41 | 92.23     | 85.21  |
|       | kNN        | **94.53** | 94.80 | 94.52     | 89.60  |
|       | GNB        | 68.22 | 68.22 | 62.71     | 43.22  |
|       | LR         | 71.61 | 71.61 | 70.14     | 51.04  |
|       | MLP        | **90.36** | 90.32 | 91.00     | 81.70  |
|       | ELM        | **90.36** | 90.36 | 90.29     | 81.66  |
|       | CC-ELM     | **91.40** | 91.45 | 90.96     | 83.63  |
| SET-3 | SVM        | **95.31** | 95.35 | 95.54     | 90.93  |
|       | kNN        | **94.79** | 94.90 | 95.00     | 90.03  |
|       | GNB        | 60.67 | 61.87 | 65.33     | 46.00  |
|       | LR         | 71.61 | 71.48 | 73.35     | 51.06  |
|       | MLP        | 80.98 | 81.03 | 80.43     | 65.66  |
|       | ELM        | **97.39** | 97.37 | 97.30     | 94.82  |
|       | CC-ELM     | **91.92** | 91.91 | 91.73     | 84.47  |
| SET-4 | SVM        | 84.63 | 84.65 | 84.68     | 71,65  |
|       | kNN        | 84.89 | 84.90 | 85.05     | 72,08  |
|       | GNB        | 56.77 | 56.95 | 59.28     | 37,74  |
|       | LR         | 55.46 | 55.53 | 53.91     | 30,66  |
|       | MLP        | 65.10 | 64.89 | 68.69     | 41,09  |
|       | ELM        | 82.55 | 82.51 | 81.34     | 68.09  |
|       | CC-ELM     | 73.43 | 73.45 | 73.44     | 53.94  |
| SET-5 | SVM        | **92.70** | 92.52 | 92.05     | 85.49  |
|       | kNN        | **95.57** | 95.52 | 95.29     | 91.23  |
|       | GNB        | 65.88 | 65.15 | 58.68     | 40.47  |
|       | LR         | 71.61 | 71.19 | 67.85     | 50.05  |
|       | MLP        | 66.92 | 66.30 | 60.92     | 42.55  |
|       | ELM        | **90.62** | 90.66 | 90.32     | 82.04  |
|       | CC-ELM     | 79.68 | 79.60 | 78.45     | 63.20  |

Table 4: Classification performance results with respect to FSC estimations with AE at EC state

|  | Classifier | CA | AUC | F1- score | G-mean |
|---|---|---|---|---|---|
| SET-1 | SVM | **97.39** | 97.37 | 97.31 | 94.80 |
|  | kNN | **97.91** | 97.88 | 97.83 | 95.78 |
|  | GNB | 65.36 | 66.55 | 75.25 | 59.59 |
|  | LR | **90.62** | 90.65 | 90.86 | 82.17 |
|  | MLP | **93.48** | 93.38 | 93.03 | 87.13 |
|  | ELM | **98.17** | 98.12 | 98.25 | 96.26 |
|  | CC-ELM | **99.47** | 99.44 | 99.44 | 98.88 |
| SET-2 | SVM | **95.83** | 95.83 | 95.94 | 91.83 |
|  | kNN | **97.13** | 97.12 | 97.22 | 94.33 |
|  | GNB | 57.03 | 57.76 | 68.13 | 48.50 |
|  | LR | 68.22 | 68.33 | 68.06 | 46.61 |
|  | MLP | 75.00 | 75.04 | 74.05 | 56.12 |
|  | ELM | **93.48** | 93.33 | 94.00 | 87.06 |
|  | CC-ELM | **87.76** | 87.78 | 87.53 | 76.99 |
| SET-3 | SVM | **96.35** | 96.39 | 96.20 | 92.92 |
|  | kNN | **96.61** | 96.59 | 96.42 | 93.30 |
|  | GNB | 72.13 | 71.69 | 68.25 | 50.67 |
|  | LR | 82.55 | 82.54 | 81.74 | 68.14 |
|  | MLP | 84.89 | 84.52 | 82.94 | 71.25 |
|  | ELM | **96.09** | 96.09 | 96.22 | 92.35 |
|  | CC-ELM | **94.27** | 94.37 | 94.30 | 88.99 |
| SET-4 | SVM | **88.28** | 88.29 | 88.43 | 77.92 |
|  | kNN | **86.97** | 86.98 | 87.18 | 75.63 |
|  | GNB | 63.02 | 63.09 | 67.28 | 38.02 |
|  | LR | 63.80 | 63.82 | 65.16 | 40.56 |
|  | MLP | 67.44 | 66.91 | 71.40 | 43.71 |
|  | ELM | 82.29 | 82.30 | 82.29 | 67.73 |
|  | CC-ELM | 77.60 | 77.13 | 80.00 | 59.15 |
| SET-5 | SVM | **91.40** | 91.61 | 91.47 | 83.77 |
|  | kNN | **92.96** | 93.09 | 93.13 | 86.61 |
|  | GNB | 60.93 | 61.67 | 60.23 | 39.79 |
|  | LR | 67.96 | 68.43 | 66.12 | 46.02 |
|  | MLP | 80.20 | 80.15 | 78.89 | 63.95 |
|  | ELM | 84.37 | 84.62 | 71.42 | 84.46 |
|  | CC-ELM | 84.11 | 83.84 | 82.42 | 69.98 |
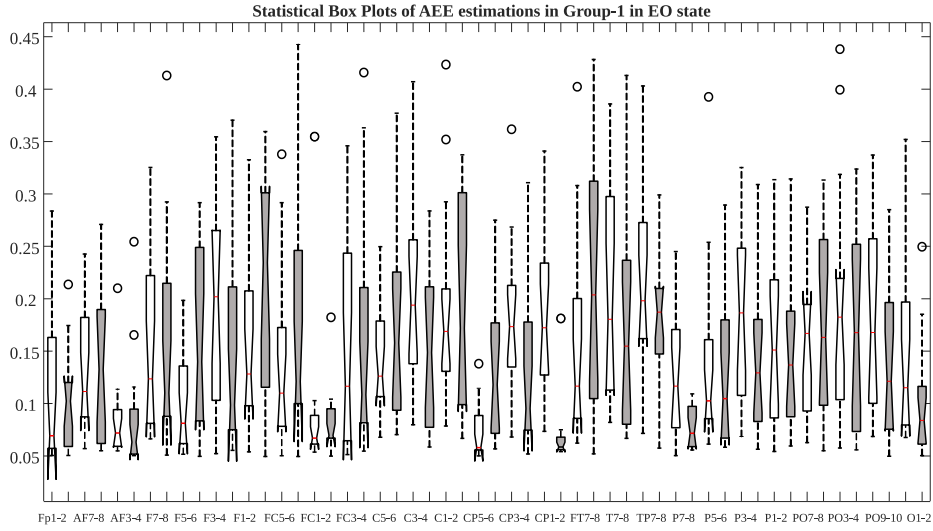
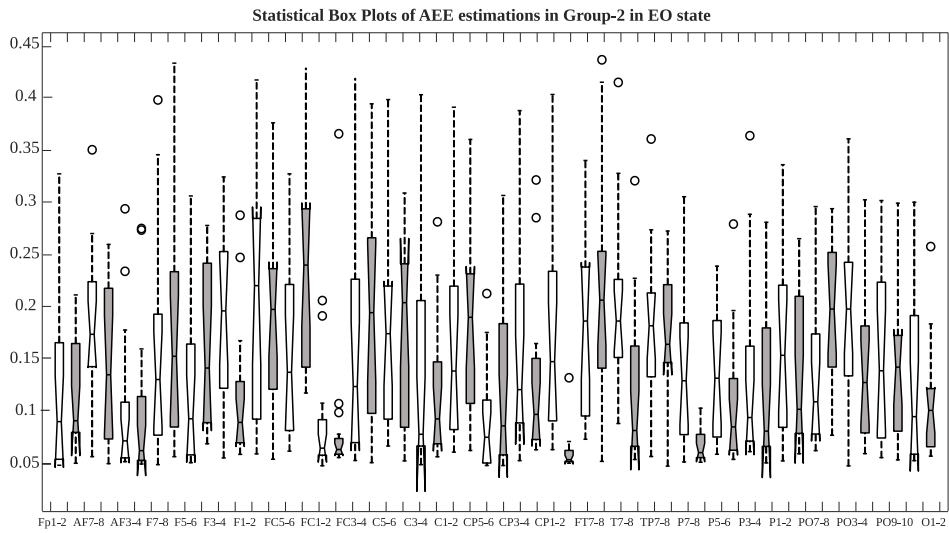Figure 3: Statistical box plots of FSC estimations with AE in EO state in Group-1



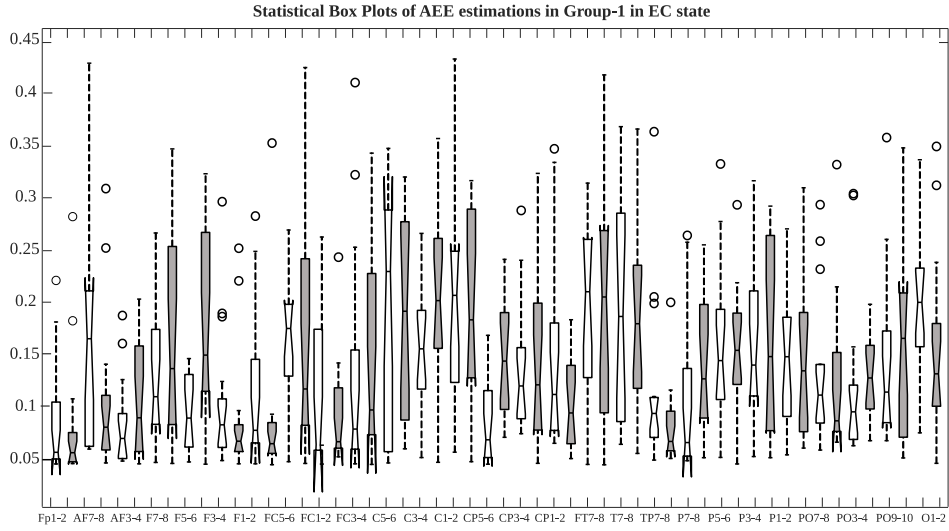Figure 4: Statistical box plots of FSC estimations with AE in EO state in Group-2

Figure 5: Statistical box plots of FSC estimations with AE in EC state in Group-1
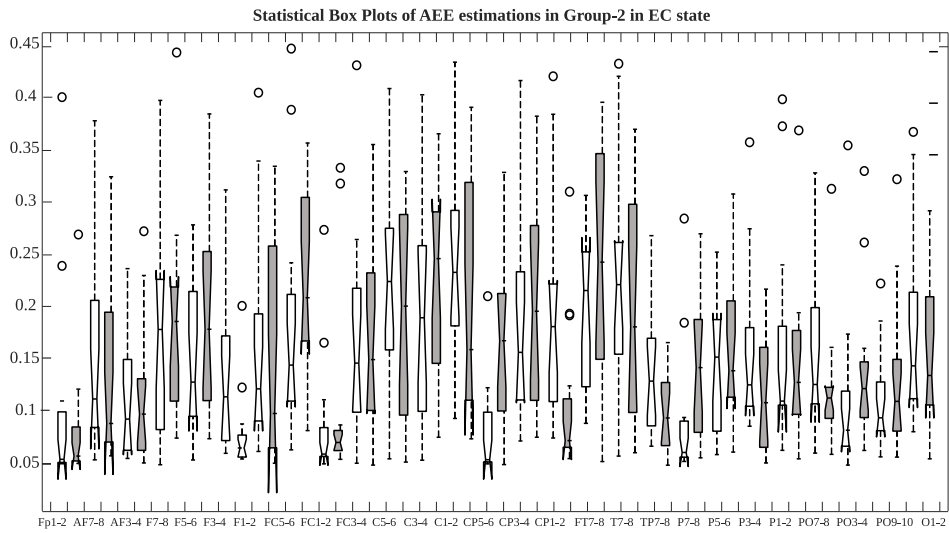


Figure 6: Statistical box plots of FSC estimations with AE in EC state in Group-2

Table 5: Statistical p-values between groups in both EC and EO states in accordance with FSC estimations with AE (statistically meaningful level is $p < 0.05$)

| channel | EC | EO | channel | EC | EO |
|---------|------|------|---------|------|------|
| Fp1 | 0.079 | 0.085 | PO10 | 0.043* | 0.011* |
| Fp2 | 0.090 | 0.092 | AF7 | 0.058 | 0.071 |
| F7 | 0.068 | 0.0009* | AF3 | 0.084 | 0.070 |
| F3 | 0.085 | 0.005* | AF4 | 0.063 | 0.091 |
| Fz | 0.016* | 0.047* | AF8 | 0.024* | 0.070 |
| F4 | 0.096 | 0.038* | F5 | 0.087 | 0.087 |
| F8 | 0.009* | 0.034* | F1 | 0.052 | 0.015* |
| FC5 | 0.097 | 0.048* | F2 | 0.060 | 0.051 |
| FC1 | 0.026* | 0.077 | F6 | 0.024* | 0.054 |
| FC2 | 0.001* | 0.001* | FT7 | 0.025* | 0.056 |
| FC6 | 0.061 | 0.074 | FC3 | 0.022* | 0.011* |
| T7 | 0.072 | 0.050 | FC4 | 0.003* | 0.005* |
| C3 | 0.016* | 0.004* | FT8 | 0.090 | 0.090 |
| Cz | 0.009* | 0.057 | C5 | 0.074 | 0.030* |
| Veog | 0.001* | 0.002* | C1 | 0.016* | 0.008* |
| C4 | 0.040* | 0.029* | C2 | 0.085 | 0.024* |
| T8 | 0.075 | 0.008* | C6 | 0.066 | 0.012* |
| CP5 | 0.036* | 0.006* | TP7 | 0.043* | 0.091 |
| CP1 | 0.0002* | 0.005* | CP3 | 0.029* | 0.061 |
| CP2 | 0.0009* | 0.015* | CPz | 0.022* | 0.010* |
| CP6 | 0.005* | 0.038* | CP4 | 0.087 | 0.030* |
| Afz | 0.099 | 0.057 | TP8 | 0.030* | 0.076 |
| P7 | 0.079 | 0.006* | P5 | 0.046 | 0.0044* |
| P3 | 0.016* | 0.019* | P1 | 0.046 | 0.036* |
| Pz | 0.040* | 0.015* | P2 | 0.018* | 0.029* |
| P4 | 0.003* | 0.009* | P6 | 0.043* | 0.024* |
| P8 | 0.069 | 0.014* | PO7 | 0.079 | 0.035* |
| PO9 | 0.083 | 0.075 | PO3 | 0.081 | 0.011* |
| O1 | 0.092 | 0.065 | POz | 0.054 | 0.002* |
| Oz | 0.035* | 0.071 | PO4 | 0.050 | 0.037* |
| O2 | 0.030* | 0.010* | PO8 | 0.001* | 0.054 |
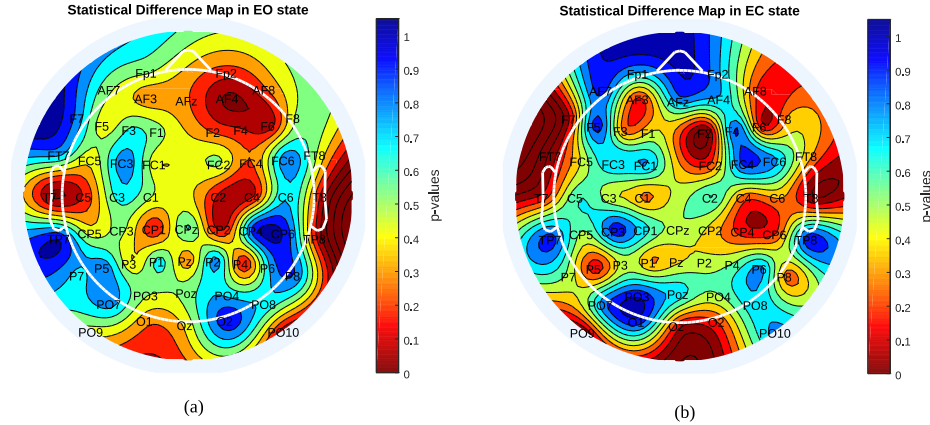
Figure 7: Cortical difference maps between the groups in EO (a) and EC (b) states (colour bar is correlated with 0.1x(p-values))

## 6. Conclusion and Discussion

In the present study, a new indicator so called FSC has been proposed for classification of maladaptive rumination in resting-state, since electrophysiological findings commonly reveal close relations between mental disorders and neuro-functional network across the whole cortex even in the resting state [100, 101, 102]. Usefulness of WE and AE in computing frequency band specific EEG complexity is tested for estimation of accurate FSC. Then, the reliability of FSC is tested by examining supervised machine learning models and extreme learning machines for detection of maladaptive rumination from resting-state EEG recordings. In addition, statistical differences between the groups are computed through one-way Anova tests according to the corresponding best results.

AE provided considerable better estimations in comparison to WE due to nonlinear nature of EEG segments. AE is a nonlinear statistical quantity of signal irregularity such that its performance depends on the largeness of time-series. Comparison of AE with WE has been studied in EEG analysis with several goals such as detection of driving fatigue [103, 104] and seizure [105].

Alpha and Beta sub-band specific complexity estimations are averaged to provide FSC in resting-state, since EEG analysis has frequently focused on Alpha and Beta sub-bands for estimation of cognitive skills in resting-state in both past and recent studies [106, 107, 108, 109]. Multi-channel FSC estimations are considered as separate instants (i.e. features) in two-class classification steps. Dimension of the features is identical to the number recording channels that are included in regional features such SET-2, SET-3, SET-4 and SET-5. So, the largest feature set is SET-1 including FSC values estimated from 62-channels

19

over a 1 $min$ duration trial divided into short segments of 2 $sec$ according to 20 individuals in each group. As the number of recording channels increases, both dimension and number of the features also increases in feature sets. Therefore, the best classification performance is obtained through 5-fold cross validated CCR-ELM driven by the largest feature set including FSC values estimated with AE at EC state. In addition to higher CA, CCR-ELM is also faster than the other machine learning models. It can be stated that the classification performance is decreased as the number of features is decreased, however, FSC values estimated with AE are able to detect neuro-functional complexity differences originated from maladaptive rumination at both states (EC, EO) in each feature set classified by any classifier except GNB. In reference study, GNB was reported as less successful than both SVM and k-NN [84].

In conclusion, the results reveal that maladaptive rumination is highly relevant to FSC estimations (averaged EEG complexity with AE in Alpha and Beta sub-bands of short EEG segments) at mostly EC state at mostly frontal, centro-parietal and parietal locations. In detail, FSC values are decreased in maladaptive ruminations characterized by repetitive thoughts associated with negative feelings. In literature, the left frontal cortex is assumed to be responsible for management of arousal and regulation of stress response, while the right frontal cortex was reported to manage the fight or flight response [86]. However, the current results prove that the whole cortex is more or less affected by cognitive abilities in management of negative emotions. Since, the people with a high tendency to rumination have low ability to manage negative emotions, it is the important issue to correlate maladaptive rumination with resting-state EEG based quantitative indicators.

Since, frequently use of negative ERS called rumination induces deficits in cognitive functioning, the most important hallmark symptoms of major depression disorder, wherein individuals retrieve and repetitively rehearse autobiographical and negatively valance content about both past and current issues [110, 111]. Moreover, persons who use frequently rumination in daily life, have trouble with sustained attention. Thus, maladaptive rumination is one of the most problematic cognitive symptoms in adults. The present study propose a new quantitative tool to understand the neural mechanism underlying repetitive negative thoughts triggered by depressive feelings.

**Conflict of Interest**

The authors declare that they have no conflict of interest.

**References**

[1] Park, Y., Chung, W. (2020) A novel EEG correlation coefficient feature extraction approach based on demixing EEG channel pairs for cognitive task classification, IEEE Access, doi:10.1109/ACCESS.2020.2993318

[2] Lee, D.H., Jeong, J.H., et al. (2020) Continuous EEG decoding of pilots' mental states using multiple feature block-based convolutional neural network, IEEE Access, doi:10.1109/ACCESS.2020.3006907.

[3] Wu, D., Xu, Y., Lu, B.L. (2020) Transfer learning for EEG-based brain-computer interfaces: A review of progress made since 2016, IEEE Trans on Cogn. and Dev. Sys., doi:10.1109/TCDS.2020.3007453.

[4] Aslam, AR et al., (2020) An on-chip processor for chronic neurological disorders assistance using negative affectivity classification, IEEE Trans on Biom. Circ. and Sys., 14(4):838-851.

[5] Aslam, A.R., Altaf, MAB (2021) A 10.13μJ/Classification 2-channel deep neural network based SoC for negative emotion outburst detection of autistic children, in IEEE Trans on Bio. Circ. and Sys., 15(5):1039-1052.

[6] Fadlallah, B., Seth, S., et al. (2012) Quantifying cognitive state from EEG using dependence measures, IEEE Trans on BME, doi:10.1109/TBME.2012.2210283.

[7] Mullen, T.R., Kothe, C.A.E., et al. (2015) Real-time neuroimaging and cognitive monitoring using wearable dry EEG, IEEE Trans on BME, doi:10.1109/TBME.2015.2481482.

[8] Paranjape, P.N., Dhabu, M.M., et al. (2019) Cross-correlation aided ensemble of classifiers for BCI oriented EEG study, IEEE Access, doi10.1109/ACCESS.2019.2892492

[9] Chen,J.X., et al. (2019) A hierarchical bidirectional GRU model with attention for EEG-based emotion classification, IEEE Access, doi:10.1109/ACCESS.2019.2936817.

[10] Torres, E.P., et al. (2020) EEG-based BCI emotion recognition: A survey, Sensors, 20(18):5083.

[11] Yannick R. et al (2019) Deep learning-based electroencephalography analysis: a systematic review, J of Neur. Eng., doi:10.1088/1741-2552/ab260c

[12] Wu, D., Lance, B.J., Lawhern, V.J. (2017) EEG-based user reaction time estimation using riemannian geometry features, IEEE Trans on Neu. Sys. and Rehab. Eng., 25(11):2157–2168.

[13] Hu, B., Li, X., Sun, S., Ratcliffe, M. (2018) Attention recognition in EEG-based affective learning research using CFS+KNN algorithm, IEEE/ACM Trans on Comp. Biology and Bioinformatics, 15(1):38–45.

[14] Qian, D., Wang, B., Qing, X. et al. (2017) Drowsiness detection by bayesian-copula discriminant classifier based on EEG signals during daytime short nap, IEEE Trans on BME, 64(4):743–754.

[15] Durongbhan, P., Zhao, Y., et al. (2019) A dementia classification framework using frequency and time-frequency features based on EEG signals, IEEE Trans on Neu. Sys. and Rehab. Eng., 27(5):826–835.

[16] van Diessen, E., Numan, T., et al. (2015) Opportunities and methodological challenges in EEG and MEG resting state functional brain network research, Clin. Neuroph., doi:10.1016/j.clinph.2014.11.018.

[17] Bartolomei, F. et al. (2005) Acute alteration of emotional behaviour in epileptic seizures is related to transient desynchrony in emotion-regulation networks, Clin. Neurophysiol., 116(116):2473-2479.

[18] Ochsner, K.N., Gross, J.J. (2008) Cognitive emotion regulation: insights from social cognitive and affective neuroscience, Current Directions in Psychological Science, 17:153–158.

[19] Gross, J.J. (2002) Emotion regulation: affective, cognitive, and social consequences, Psychophy., 39(3):281-91.

[20] Phan,K.L., Fitzgerald, D.A., et al. (2005) Neural substrates for voluntary suppression of negative affect: a functional magnetic resonance imaging study, Biol. Psych., 57:210—219.

[21] Webb, T.L., Miles, E., Sheeran, P. (2012) Dealing with feeling: a meta-analysis of the effectiveness of strategies derived from the process model of emotion regulation, Psychol. Bull., 138(4):775-808.

[22] Goldin,P.R., et al. (2008) The neural bases of emotion regulation: reappraisal and suppression of negative emotion, Biological Psychiatry, 63:577–586.

[23] Babayan, A. Erbey, M. Kumral, D. et al. (2019) Data Descriptor: A mindbrainbody dataset of MRI, EEG, cognition, emotion, and peripheral physiology in young and old adults, Scientific Data, 6(1):180308.

[24] Robert J. Barry, Adam R., et al. (2007) EEG differences between eyesclosed and eyes-open resting conditions, Clin. Neurophy., 118(12):2765-2773.

[25] Barry RJ, et al. (2009) EEG differences in children between eyes-closed and eyes-open resting conditions, Clin. Neurophy., doi:10.1016/j.clinph.2009.08.006.

[26] Babiloni, C., Lizio, R., et al. (2010) Reactivity of cortical alpha rhythms to eye opening in mild cognitive impairment and Alzheimer's disease: an EEG study, J. of Alzheimer's disease, doi:10.3233/JAD-2010-100798

[27] Kropotov, J.D. (2016) Functional neuromarkers for psychiatry, App. for Diag. and Treat., Part5-6, doi:10.1016/C2012-0-07144-X, Elsevier press.

[28] van Elst, L.T., Woermann, L.G., et al. (2000) Affective aggression in patients with temporal lobe epilepsy, A quantitative MRI study of the amygdala, Brain, doi:10.1093/brain/123.2.234.

[29] Gotman, J. (2008) Epileptic networks studied with EEG-fMRI, Epilepsia, doi:10.1111/j.1528-1167.2008.01509.x

[30] Chua, R.N., Hau, Y.W., Tiew, C.M., Hau, W.L. (2019) Investigation of attention deficit/hyperactivity disorder assessment using electro interstitial scan based on chronoamperometry technique, IEEE Access, doi:10.1109/ACCESS.2019.2938095

[31] Zhao,Y., Zhao, Y., Durongbhan, P. et al. (2019) Imaging of nonlinear and dynamic functional brain connectivity based on EEG recordings with the application on the diagnosis of Alzheimer's disease, IEEE Trans on Med. Imag., doi10.1109/TMI.2019.2953584.

[32] Sharma, P., Khan, Y.U., et al. (2014) A wavelet-statistical features approach for non-convulsive seizure detection, Clin. EEG and Neuro., 45(4):274–284.

[33] Cura, O.K., Akan, A. (2020) Classification of epileptic EEG signals using synchrosqueezing transform and machine learning, Int J Neural Syst., doi:10.1142/S0129065721500052

[34] Ma, X., Yu, N., Zhou, W. (2019) Using dictionary pair learning for seizure detection, Int J Neural Syst., doi:10.1142/S0129065718500053

[35] Tapani, K.T., Vanhatalo, S., Stevenson, N.J. (2019) Time-varying EEG correlations improve automated neonatal seizure detection, Int J Neural Syst., doi:10.1142/S0129065718500302.

[36] Haghighi, M., Moghadamfalahi, M., et al. (2017) A graphical model for online auditory scene modulation using EEG evidence for attention, IEEE Trans on Neu. Sys. and Rehab. Eng., 25(11):1970–1977.

[37] Myrden, A., Chau, T. (2017) A passive EEG-BCI for single-trial detection of changes in mental state, IEEE Trans on Neu. Sys. and Rehab. Eng., 25(4):345–356.

[38] Jiahui, P., Qiuyou, X., et al. (2018) Emotion-related consciousness detection in patients with disorders of consciousness through an EEG-based BCI system, Front. in Hum. Neuro., 12:198.

[39] Barry, R.J., Clarke, A.R., et al.(2007) EEG differences between eyes-closed and eyes-open resting conditions. Clin Neuroph., doi:10.1016/j.clinph.2007.07.028.

[40] Greer, J.M.H., Riby, D.M., et al. (2012) An EEG investigation of alpha and beta activity during resting states in adults with Williams syndrome. BMC Psychol, doi:10.1186/s40359-021-00575-w

[41] Newson, J.J., Thiagarajan, T.C. (2019) EEG Frequency Bands in Psychiatric Disorders: A Review of Resting State Studies, Front. Hum. Neurosci., doi:10.3389/fnhum.2018.00521

[42] Thul, A., Lechinger, J. et al. (2016) EEG entropy measures indicate decrease of cortical information processing in disorders of consciousness, Clinical Neurophysiology, 127(2):1419–1427.

[43] Engemann, D.A., Raimondo, F. et al. (2018) Robust EEG-based cross-site and cross-protocol classification of states of consciousness, Brain, 141(11):3179–3192.

[44] José, A., et al. (2019) Differential effects of simulated cortical network lesions on synchrony and EEG complexity, Int. J. of Neural Systems, 29(04):1850024.

[45] Miskovic, V., MacDonald, K.J., et al. (2019) Changes in EEG multiscale entropy and power-law frequency scaling during the human sleep cycle, Human Brain Mapping, 40(2):538–551.

[46] Garcia-Martinez, B., et al. (2016) Application of entropy-based metrics to identify emotional distress from electroencephalographic recordings, Entropy, 18(6):221.

[47] Garcia-Martinez, B., et al. (2020) Recognition of emotional states from EEG signals with nonlinear regularity and predictability-based entropy metrics, Cogn. Comp., doi:10.1007/s12559-020-09789-3.

[48] Li, L., Chen, W., Shao, X., Wang, Z. (2010) Analysis of amplitude-integrated EEG in the newborn based on approximate entropy, IEEE Trans on BME, 57(10):2459–2466.

[49] Cheng, Q., Yang, W., et al. (2019) Increased sample entropy in EEGs during the functional rehabilitation of an injured Brain, Entropy, 21(7):698.

[50] Cubero, J.A., Gan, J.Q., Palaniappan, R. (2013) Multiresolution analysis over simple graphs for brain computer interfaces, J. of Neural Eng., 10(4):046014.

[51] Aydın, S., Arıca, N., et al., (2015) Classification of obsessive compulsive disorder by EEG complexity and hemispheric dependency measurements, Int. J. of Neu. Sys., 25(3):155001.

[52] Zandi, A.S., Javidan, M., Dumont, G.A. et al. (2010) Automated real-time epileptic seizure detection in scalp EEG recordings using an algorithm based on wavelet packet transform, IEEE Trans on BME, doi10.1109/TBME.2010.2046417.

[53] Khatun, S., Mahajan, R., Morshed, B.I. (2016) Comparative study of wavelet-based unsupervised ocular artifact removal techniques for single-channel EEG data, IEEE J. of Trans. Eng. in Health and Med., doi:10.1109/JTEHM.2016.2544298

[54] Guo, C., Yu, J., Wu, L., et al. (2019) Analysis and feature extraction of EEG signals induced by anesthesia monitoring based on wavelet transform, IEEE Access, doi10.1109/ACCESS.2019.2907794

[55] Xu, X., Zhang, Y., Tang, M. et al. (2020) Emotion recognition based on double tree complex wavelet transform and machine learning in internet of things, IEEE Access, doi:10.1109/ACCESS.2019.2948884

[56] Pitchford, B., Arnell, K.M. (2019) Resting EEG in alpha and beta bands predicts individual differences in attentional breadth, Conscious. and Cogn., 75:102803

[57] Aydın, S., Demirtaş, A. Tunga, et al. (2018). Comparison of hemispheric asymmetry measurements for emotional recordings from controls, Neural Comput & Applic., 30:1341-–1351.

[58] Yuvaraj, R., Murugappan, M., et al. (2014). Emotion classification in Parkinson's disease by higher-order spectra and power spectrum features using EEG signals, A comparative study, J. of Integrative Neuro., 13(1):89-120.

[59] Zheng, W.L., Lu, B.L. (2015). Investigating critical frequency bands and channels for EEG based emotion recognition with deep neural networks, IEEE Trans on Auto. Mental Devel., 7(3):162–175.

[60] Mardini, W., Yassein, M.M.B., Al-Rawashdeh, R. et al. (2020) Enhanced detection of epileptic seizure using EEG signals in combination with machine learning classifiers, IEEE Access, doi:10.1109/ACCESS.2020.2970012.

[61] Yao, W., Siyu, J., Tianshun, Y. et al. (2020) An efficient method to detect sleep hypopneaapnea events based on EEG signals, IEEE Access, doi:10.1109/ACCESS.2020.3038486.

[62] Sharmila, A., Greethanjali, P. (2016) DWT based detection of epileptic seizure from EEG signals using naive bayes and k-NN classifiers, IEEE Access, doi:10.1109/ACCESS.2016.2585661

[63] Gotlib IH, Joormann J. (2010) Cognition and depression: Current status and future directions. Ann. Rev. of Clin. Psych. 6:285–312

[64] Crespel, A., Gelisse, P., et al. (2005) Atlas of Electroencephalography, vol.1, J. Libbey Eurotext, Paris, France, 1st ed.

[65] Vigon, L., Saatchi, M.R., et al. (2000) Quantitative evaluation of techniques for ocular artefact filtering of EEG waveforms, IEE Proc.of Science, Measurement and Tech., 147(5):219–228, 2000.

[66] Mohammadi, A., Zahiri, S.H. et al. (2021) Design and modeling of adaptive IIR filtering systems using a weighted sum - variable length particle swarm optimization, *App. Soft Comp.*, doi:10.1016/j.asoc.2021.107529.

[67] Rajaguru, H., Prabhakar, S.K. (2017) Logistic regression Gaussian mixture model and softmax discriminant classifier for epilepsy classification from EEG signals, Int. Conf. on Comp. Methodologies and Communication (ICCMC), doi10.1109/ICCMC.2017.8282615.

[68] Ronquillo, L.H., Adams, S. et al. (2018) Epilepsy in an elderly population: Classification, etiology and drug resistance, Epilepsy Research, 140:90–94.

[69] Chao, P., Cheng, S., Honglang, M., et al. (2020). EEG-based emotion recognition using logistic regression with gaussian kernel and laplacian prior and investigation of critical frequency bands, App. Sci., doi:10.3390/app10051619.

[70] Yasuda, W., Aihara, T. et al. (2010). Brain imaging of motor control activity using EEG and a combination of hierarchical variational bayesian method and sparse logistic regression, Neuro. Res., 68, Supp.1, e332

[71] Ieracitano, C., et al. (2020) A novel multi-modal machine learning based approach for automatic classification of EEG recordings in dementia, Neural Networks, doi:10.1016/j.neunet.2019.12.006.

[72] Abbasi, SF., Ahmad, J., et al. (2020) EEG-based neonatal sleep-wake classification using multilayer perceptron neural network, IEEE Access, doi:10.1109/ACCESS.2020.3028182

[73] Dreiseitla, S., Ohno-Machadob, L. (2002). Logistic regression and artificial neural network classification models: a methodology review, J. of Biomed. Informatics, 35(5–6):352–359.

[74] Garnefski, N., et al. (2001) Negative life events, cognitive emotion regulation and emotional problems, Pers. Individ. Dif, 30:1311–1327.

[75] Pincus, S. (1991) Approximate entropy as a measure of system complexity, Proc. Nati. Acad. Sci. Mathematics, USA, 88:2297–2301.

[76] Pincus SM. Assessing serial irregularity and its implications for health. Ann NY Acad Sci 2001, 954:245–67.

[77] Richman, JS., Moorman, J.R. (2000) Physiological time-series analysis using approximate entropy and sample entropy, Amer. J. of Phys., doi:10.1152/ajpheart.2000.278.6.H2039

[78] Kennel, MB., Brown, R., Abarbanel, H.D.I. (1992) Determining embedding dimension for phase-space reconstruction using a geometrical construction, Phys. Rev. A, Gen. Phys., 45:3403–3411.

[79] Rosso OA, Blanco S, et al. (2001) Wavelet entropy: a new tool for analysis of short duration brain electrical signals. J Neurosci Meth., doi:10.1016/s0165-0270(00)00356-3.

[80] Daubechies, I. (1992) Ten lectures on wavelets. Philadelphia, PA: Society for Industrial and Applied Mathematics.

[81] Orosco, L., Correa, A.G., Laciar, E. (2013) Review: A survey of performance and techniques for automatic epilepsy detection, J. Med. Biol. Eng., 33(6):526–537.

[82] Sarkela, M.O.K., Ermes, M.J., et al. (2007). Quantification of epileptiform electroencephalographic activity during sevoflurane mask induction. Anesthesiology, 107:928–938, doi:10.1097/01.

[83] Xiao, W., Zhang, J. et al. (2017) Class-specific cost regulation extreme learning machine for imbalanced classification, Neurocomp., doi:10.1016/j.neucom.2016.09.120.

[84] Aydın, S., Güdücü, Ç., et al. (2019) The impact of musical experience on neural sound encoding performance. Neurosci Lett., doi:10.1016/j.neulet.2018.11.034.

[85] Powers, D.M.W. (2011) Evaluation: From precision, recall and F-measure to ROC, informedness, markedness and correlation, J. of Mach. Lear. Tech., 2(1):37–63.

[86] Craig, A.D. (2005) Forebrain emotional asymmetry: a neuroanatomical basis? Trends in Cogn. Science, 9(12):566–571.

[87] Ingram, R.E. (1990) Self-focused attention in clinical disorders: review and a conceptual model, Psycho. Bull., 109:156-176

[88] Nolen-Hoeksema, S. (2000) The role of rumination in depressive disorders and mixed anxiety/depressive symptoms, J. of Abn. Psych., 109:504-511

[89] Spasojevic, J., Alloy, L.B. (2001) Rumination as a common mechanism relating depressive risk factors to depression, Emotion, 1:25-37

[90] Nolen-Hoeksema, S., et al.(2008) Rethinking rumination, Perspect. Psychol. Sci., 3(5):400-424.

[91] Drost, J., Does, W. et al. (2014) Repetitive negative thinking as a transdiagnostic factor in depression and anxiety: a conceptual replication, Behav. Res. Ther., 63:177-183.

[92] Harrington J.A., Blankenship, V. (2002) Ruminative thoughts and their relation to depression and anxiety. J. of App. Soc. Psych., 32(3):465-485.

[93] Mayou, R.A., Ehlers, A., Bryant, B. (2002) Posttraumatic stress disorder after motor vehicle accidents: 3-year follow-up of a prospective longitudinal study, Behav. Res. Ther., 40(6):6

[94] Yu S.H., Tseng C.Y., Lin W.L. (2020) A neurofeedback protocol for executive function to reduce depression and rumination: A Controlled Study. Clin Psychop. Neuro., 18(3):375-385.

[95] Ferdek, M.A., et al. (2016) Depressive rumination and the emotional control circuit: An EEG localization and effective connectivity study. Cogn Affect Behav Neurosci, doi:10.3758/s13415-016-0456-x

[96] Andersen, S.B., Moore, R.A., et al.(2009) Electrophysiological correlates of anxious rumination. Int J Psychophysiol, 71(2):156-69, doi:10.1016/j.ijpsycho.2008.09.004.

[97] Pan D.N., Hoid D., Gu R.L., Li X. (2020) Emotional working memory training reduces rumination and alters the EEG microstate in anxious individuals. Neuroimage Clin. doi:10.1016/j.nicl.2020.102488.

[98] Rosenbaum, D., Kroczek, A.M., al. (2020) Neural correlates of mindful emotion regulation in high and low ruminators. Sci Rep, doi:10.1038/s41598-020-71952-5.

[99] Connell, A., Danzo, S., et al. (2020) Rumination in early adolescent girls: An EEG study of cognitive control and emotional responding in an emotional Go/NoGo task. Cogn Affect Behav Neurosci. 20(1):181-194.

[100] Chang C., Liu Z.M., Chen M.C., et al. (2013) EEG correlates of time-varying BOLD functional connectivity, Neuroimage, 72:227–36.

[101] Kang J., Wang L., Yan C.G., et al. (2011) Characterizing dynamic functional connectivity in the resting brain using variable parameter regression and Kalman filtering approaches. Neuroimage, 56:1222–34.

[102] Hutchison R.M., et al. (2013) Dynamic functional connectivity: promise, issues, and interpretations. Neuroimage, 80:360–78.

[103] Zhang, C., Wang, H., Fu R. (2014) Automated Detection of Driver Fatigue Based on Entropy and Complexity Measures, IEEE Trans on Intell. Trans. Sys., doi:10.1109/TITS.2013.2275192.

[104] Chuckravanen, D. (2014) Approximate Entropy as a measure of cognitive fatigue: An EEG pilot study, Int. J. of Emerg. Trends in Sci. and Tech., 01(07):1036-1042.

[105] Guo L, Rivero D, Pazos A. (2010) Epileptic seizure detection using multiwavelet transform based approximate entropy and artificial neural networks. J Neurosci Methods. 193(1):156-63.

[106] Jann K, Koenig T, Dierks T, et al. (2010) Association of individual resting state EEG alpha frequency and cerebral blood flow. Neuroimage. 51(1):365-72. doi:10.1016/j.neuroimage.2010.02.024.

[107] Koelewijn L, Bompas A, Tales A, et al. (2017) Alzheimer's disease disrupts alpha and beta-band resting-state oscillatory network connectivity. Clin Neurophysiol. 128(11):2347-2357.

[108] Greer JMH, Riby DM, et al. (2021) An EEG investigation of alpha and beta activity during resting states in adults with Williams syndrome. BMC Psychol. 9(1):72.

[109] Fodor Z, Horváth A, et al. (2021) EEG alpha and beta band functional connectivity and network structure mark hub overload in Mild Cognitive Impairment during memory maintenance. Front Aging Neurosci. doi:10.3389/fnagi.2021.680200.

[110] American Psychiatric Association. (2000). Diagnostic and Statistical Manual of Mental Disorders. Washington, DC: American Psych.Assoc..

[111] Davidson, R.J., Pizzagalli, et al. (2002) Depression: perspectives from affective neuroscience, Annu Rev Psychol., 53:545–574.

[112] J. Zhang, W. Xiao, Y. Li, S. Zhang (2018) Residual compensation extreme learning machine for regression, Neurocomputing, doi:10.1016/j.neucom.2018.05.057

[113] J. Zhang, Y. Li, W. Xiao, Z. Zhang (2020) Non-iterative and fast deep learning: Multilayer extreme learning machines, J. of the Franklin Ins., doi:10.1016/j.jfranklin.2020.04.033.